ACS APPLIED MATERIALS & INTERFACES

Research Article

www.acsami.org

Effects of Surface Modification on Dye-Sensitized Solar Cell Based on an Organic Dye with Naphtho[2,1-b:3,4-b′]dithiophene as the Conjugated Linker

Xiaoxu Wang,[†] Lei Guo,[‡] Ping Fang Xia,[‡] Fan Zheng,[†] Man Shing Wong,*[,‡] and Zhengtao Zhu*[,†,§]

[†]Program of Nanoscience and Nanoengineering and [§]Department of Chemistry and Applied Biological Sciences, South Dakota School of Mines and Technology, Rapid City, SD 57701

[‡]Institute of Molecular Functional Materials, Department of Chemistry and Institute of Advanced Materials, Hong Kong Baptist University, Kowloon Tong, Hong Kong SAR, China

Supporting Information

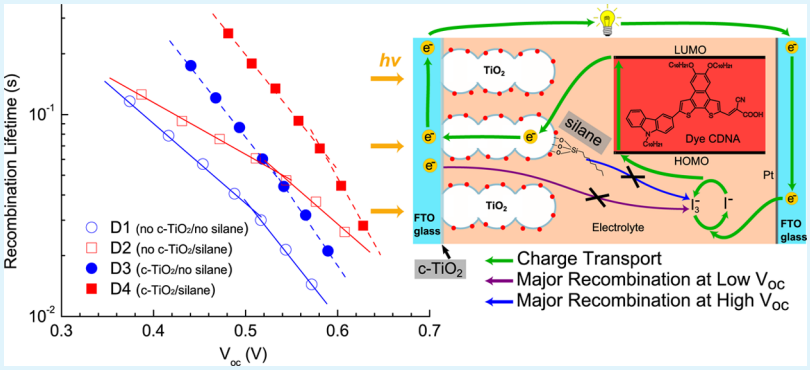

ABSTRACT: We have investigated the effects of surface modification on the dye-sensitized solar cell (DSSC) based on a donor-(π-spacer)-acceptor organic dye. A major challenge for donor−(π-spacer)−-acceptor molecules as sensitizers in DSSCs is the fast recombination reactions that occur at both the photoanode (e.g., TiO_2) surface and the fluorine-doped tin oxide (FTO) electrode, which presents unfavorable effects on the DSSC performance. The two interfaces of TiO_2/electrolyte and FTO/electrolyte are passivated selectively in a DSSC using an organic dye with Naphtho[2,1-b:3,4-b′]dithiophene as the conjugated linker and the I^-/I_3^- electrolyte. The current density−voltage characteristics, the dark current analysis, the open circuit voltage−light intensity dependence, and the transient photovoltage/photocurrent results indicate that the recombination processes are affected strongly by surface passivation under variable light intensity. At high light intensity, the recombination reaction at the TiO_2 surface is dominant. In this case, silane passivation of the TiO_2 surface can suppress recombination significantly, while the c-TiO_2 layer makes little contribution to the reduction of the recombination. At low illumination intensity, the recombination at FTO becomes significant, and the recombination can be reduced by applying a c-TiO_2 layer.

KEYWORDS: *dye-sensitized solar cell, organic dyes, electron transport, photoanode, surface passivation*

1. INTRODUCTION

Dye-sensitized solar cell (DSSC) is a promising alternative to the traditional silicon solar cell because of its low-cost nature and moderate efficiency.[1,2] In a typical DSSC, a mesoporous film of sintered TiO_2 nanoparticles sensitized with a monolayer of dye molecules serves as the photoanode. Upon light illumination, the electrons from the photoexcited dye molecules are injected and then transport through the mesoporous TiO_2 photoanode to the anode electrode (e.g., fluorine doped tin oxide (FTO)). These electrons are collected at the counter electrode through an external load, and further shuttled back to the oxidized dye molecules via redox reactions of I^-/I_3^- redox couple in the electrolyte. The dye molecules are critical to the overall device performance since they determine the amount of solar energy absorbed by the device. The common dyes in DSSCs are based on ruthenium metal−ligand complexes (e.g., N719 dye). However, the limited availability of ruthenium and the low stability of ruthenium based dyes could hinder the commercialization of DSSCs.[3] Donor-π-acceptor organic dyes, on the other hand, are promising sensitizers for DSSC application because of their high extinction coefficient and variable chemical structures for strong and broad absorption of solar energy.[3] The major challenge in utilizing organic dyes is the high recombination rate between the injected electrons and the electrolyte, which consequently lowers the open circuit voltage (V_{oc}) and the overall efficiency (η).

Received: November 6, 2013
Accepted: December 30, 2013
Published: December 30, 2013

The recombination reactions of the electrons with the electrolyte mainly occur at two places: the TiO_2 surface and the uncovered conductive FTO electrode surface.[4,5] Because the electrolyte penetrates into the mesoporous TiO_2 film, there is a great chance for recombination to take place between the electrons transporting in the TiO_2 film and the I_3^- species in the surrounding electrolyte.[6] In the meantime, the electrolyte is also in contact with the FTO electrode since the mesoporous TiO_2 film cannot completely cover the FTO surfaces; this leads to another source of recombination between the electrons in the FTO electrode and the I_3^- species in the electrolyte. Although various approaches have been used to suppress the recombination in DSSC, such as coating nanocrystalline TiO_2 film with a thin layer of a second metal oxide[7,8] or silanization,[9−11] the two recombination processes take place simultaneously in DSSCs and their contributions to the overall recombination of the device are difficult to distinguish.

In this paper, we used two surface modification methods to block the recombination at the TiO_2/electrolyte and the FTO/electrolyte interfaces in DSSCs based on a donor-π-acceptor dye (denoted as CDNA, chemical structure in Figure 1) and

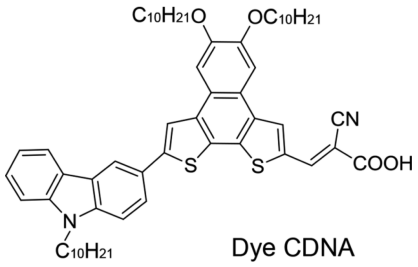

Figure 1. Chemical structure of organic dye CDNA.

the I^-/I_3^- redox couple to understand the effect of surface treatment on DSSCs based on organic sensitizer. In one passivation approach, the TiO_2 surface was modified using triethoxy(octyl)silane.[10,11] The other approach was to passivate the FTO surface using a thin compact TiO_2 blocking layer (c-TiO_2) prepared through spray pyrolysis.[12] We studied the detailed recombination loss at the TiO_2 surface and the FTO surface both separately and cooperatively in typical DSSC device structures. The current density−voltage (J−V) characterization, the open-circuit voltage (V_{oc})−light intensity (Φ_0) behavior, and the transient photocurrent and photovoltage measurements were applied to understand the electron recombination and its light intensity dependence behavior in DSSCs based on an organic sensitizer.

2. EXPERIMENTAL SECTION

2.1. Materials. Titanium(IV) oxide (P25 TiO_2) nanoparticles, triethoxy(octyl)silane, titanium di-isopropoxide bis(acetylacetonate), titanium(IV) chloride ($TiCl_4$), poly(ethylene oxide) (PEO, M_w = 35,000) and all solvents were purchased from the Sigma-Aldrich Chemical Co. The FTO glass (F-doped SnO_2, 8 Ω/□) was provided by Hartford Glass Co. The TiO_2 paste (Ti-Nanoxide T), the platinum precursor (Platisol T), the electrolyte (Iodolyte AN-50), and the spacer (Meltonix 1170−60PF) were purchased from Solaronix (Switzerland). All chemicals were used as received without further purification.

2.2. Photoanode Preparation and Surface Passivation. A TiO_2 paste composed of P25 nanoparticles and Ti-Nanoxide T was prepared first: 0.2 g of P25 nanoparticles were added into a solution of 0.2 g of ethanol, 0.5 g of water, 0.1 g of acetic acid, and 0.1 g of PEO. The paste was sonicated for 1 h to allow complete dispersion of all components. Then 0.25 g of as-prepared P25 paste was added into 0.75 g of Ti-Nanoxide T paste, followed by sonication for 1 h to yield the final TiO_2 paste. The P25 paste was used to increase the light scattering.[13]

The TiO_2 photoanode film was prepared by doctor blading of the as-prepared TiO_2 paste on the FTO glass substrate. The film was sintered at 100 °C for 30 min and then at 450 °C for 45 min. After it was cooled down to room temperature, the photoanode film was immersed in a freshly prepared 40 mM $TiCl_4$ aqueous solution at 70 °C for 30 min, and then was rinsed with deionized water and dried under N_2 flow. The $TiCl_4$-treated photoanode was sintered at 100 °C for 30 min and 450 °C for 45 min. After the photoanode was cooled down to room temperature, it was immersed in a 0.3 mM CDNA organic dye in THF solution for 18 h at room temperature. The area of the TiO_2 film was set to 0.24 cm^2 during doctor blading. The TiO_2 film thickness was measured using a Zeiss Supra 40VP field-emission scanning electron microscope (SEM).

The silane surface modification is performed immediately after dye sensitization of the TiO_2 photoanode.[10,11] 30 μL triethoxy(octyl)silane was added into 10 mL ethanol/water (v/v = 6:4) mixed solvent, followed by 1 h magnetic stir to allow complete dissolution of the silane. Then, 300 μL of acetic acid was added into the solution, followed by immersing the dye-sensitized TiO_2 photoanode film into the solution for 2 h. The film was rinsed with ethanol and dried under N_2 flow after the silane treatment.

The passivation of FTO surface was done before the preparation of the TiO_2 photoanode. The c-TiO_2 layer was coated on the conductive side of the FTO glass via spray pyrolysis of 0.2 mM titanium di-isopropoxide bis (acetylacetonate) at 200 °C for 10 cycles.[14] Prior to the spray coating, the FTO glass was cleaned in a sequence of detergent solution, deionized water, acetone, and isopropanol for 15 min each under sonication. The c-TiO_2 layer thickness was estimated by SEM.

2.3. Cell Fabrication. The DSSC fabrication followed a procedure from our previous report.[15] The counter electrode was prepared by annealing Platinum precursor Platisol T on a FTO glass (with two drilled holes) at 385 °C for 15 min. The photoanode and the counter electrode were sealed together using a 60 μm thick spacer at 100 °C, followed by injection of the Iodolyte AN-50 electrolyte through the drilled holes on the counter electrode glass. Finally, the drilled holes were sealed using parafilm.

2.4. Solar Cell Characterization and Transient Photovoltage/Photocurrent Measurement. The solar cell performance was characterized using Keithley 2612 sourcemeter. A 150 W Solar Simulator (Newport Co.) incorporated with an AM 1.5 filter was used to simulate 100 mW cm^{-2} solar illumination. The light intensity was adjusted using a Hamamatsu S1133 reference cell calibrated by the National Renewable Energy Laboratory.

The recombination lifetime (τ_e) and the diffusion coefficient (D_{eff}) of the device were measured using transient photovoltage and photocurrent setup.[16,17] In brief, under open-circuit condition, a white light emitting diode (LED) array was used to establish a bias open-circuit photovoltage of the device. A red LED pulse with 300 μs pulse width flashed on the cell to give a small rise of the photovoltage. The decay of such photovoltage perturbation was recorded via an oscilloscope. The τ_e under specified bias light intensity was obtained by fitting the decay curve with a single exponential decay function.

For D_{eff} measurement, the cell was connected in series to an identical DSSC with opposite polarity under a short-circuit condition (i.e., the photoanodes of the two cells were connected and the two counter electrodes were connected). Although both cells were illuminated with the bias white light, only one cell was flashed with a red pulse. The current decay over a 50Ω resistor in series with the cell was recorded after the light pulse. The current decay was fitted using a biexponential decay function, and the fast decay component was chosen as the photocurrent response time (τ_{pc}).[18] During the photocurrent transient measurement, the injected free electrons in the TiO_2 film either transport through the external load to the counter electrode (at which they were shuttled back to the oxidized dye by electrolyte) or recombine with the I_2 species in the surrounding

electrolyte. Thus, the measured photocurrent response time (τ_{pc}) depends on both the electron transport lifetime (τ_{trans}) and the electron recombination lifetime (τ_e) according to the following equation[5,19]

$$\frac{1}{\tau_{pc}} = \frac{1}{\tau_{trans}} + \frac{1}{\tau_e}$$

Because τ_e is more than 10 times longer than τ_{pc}, the fitted values of τ_{pc} can be considered as the electron transport lifetimes (τ_{trans}).[5,16] The diffusion coefficient was calculated using equation $D_{eff} = w^2/\tau_{trans}$, where w was the TiO_2 film thickness.[20] The diffusion length was calculated using the equation $L = (D_{eff}\tau_e)^{1/2}$.[17]

3. RESULTS AND DISCUSSION

3.1. Dye and Surface Passivation Characterization. The structure of the organic dye CDNA is shown in Figure 1. CDNA is one of the series of organic dyes based on naphthodithiophene as the π-spacer that we have recently synthesized and characterized.[21] The DSSCs based on these dyes have efficiency from 3.98 to 4.60%. The CDNA-based device has the highest efficiency of 4.60% under 100 mW AM 1.5 irradiation. Our previous studies on synthesis, physical properties, and DSSC characterization suggest that the rigid and planar structure of naphtho[2,1-b:3,4-b′]dithiophene may be a valuable spacer group in design of donor-π-acceptor molecular dyes for high-efficiency DSSCs.

CDNA is chosen in this paper since the device based on CDNA has the highest efficiency among these organic dyes with naphtho[2,1-b:3,4-b′]dithiophene motif. The HOMO and LUMO of CDNA are −5.28 eV and −3.06 eV, respectively.[21] The schematic of the relative energetics of CDNA, I^-/I_3^- redox couple, and TiO_2 photoanode is shown in Figure S1 (see the Supporting Information). The HOMO level of CDNA is ∼0.3 eV more negative than the redox potential (−4.9 eV) of I^-/I_3^- for dye regeneration, leading to relatively effective dye regeneration and moderate efficiency even without surface passivation.

The triethoxy(octyl)silane functionalization of the TiO_2 surface was characterized by FTIR spectroscopy (see the Supporting Information, Figure S2). A set of peaks were observed in the range of 2800−3000 cm^{-1}, and assigned as the typical asymmetric and symmetric stretching of the $-CH_2$ groups of the alkyl chains.[22,23] The vibration of the Si−O−Si bond was observed at ∼1035 cm^{-1}.[5] The mode at 1321 cm^{-1} was related to the Si−C bond.[20] The FTIR spectrum confirmed that the reaction of triethoxy(octyl)silane with the −OH groups on the TiO_2 surface was successful, and the alkyl chains ($-CH_2(CH_2)_6CH_3$) were attached to the TiO_2 surfaces after silane reaction.

The thickness of the TiO_2 photoanode film and the c-TiO_2 layer was evaluated using SEM (see the Supporting Information, Figure S3). The SEM image showed that the TiO_2 photoanode had typical mesoporous morphology. The TiO_2 film thickness was measured to be ∼4.5 μm. The thickness of the c-TiO_2 layer was estimated to be ∼140 nm from the SEM image.

3.2. Current Density−Voltage (*J*−*V*) Characteristics. The recombination at TiO_2 (TiO_2 surface/electrolyte interface) and FTO (FTO surface/electrolyte interface) occurs simultaneously. To get a better understanding of the behavior of the recombination reaction at each interface, we use silane treatment and c-TiO_2 layer to selectively block one or both of these recombination reaction pathways. Four types of DSSCs were fabricated and denoted as D1, D2, D3, and D4. In D1 cell, neither c-TiO_2 layer nor silane treatment was used during the fabrication, and recombination reactions at both FTO and TiO_2 took place. D2 cell had no c-TiO_2 layer, but the photoanode was passivated by silane treatment; in this case, recombination at TiO_2 would be blocked. Both D3 and D4 cells employed the c-TiO_2 layer to block the recombination at FTO; D3 had no silane treatment on the photoanode to reduce the recombination at TiO_2; the photoanode of D4 was passivated by silane and the recombination at both TiO_2 and FTO would be blocked. In one batch, two identical cells were fabricated for each type of the devices. The average of the solar cell parameters of the two identical cells and the absolute deviation were calculated. *J*−*V* curves of the DSSCs are shown in Figure 2, and the photovoltaic parameters are summarized in Table 1.

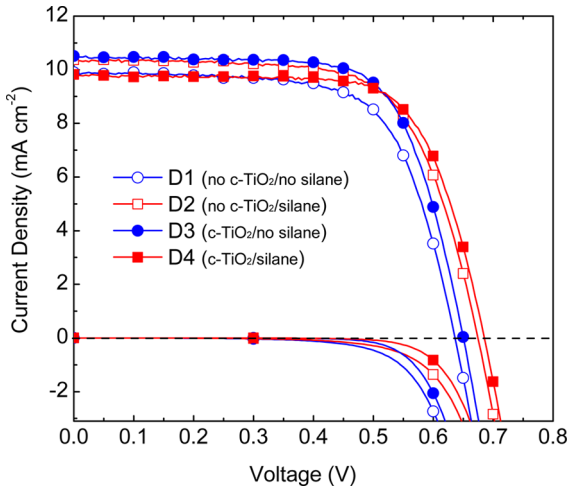

Figure 2. Current density − voltage (*J*−*V*) characteristics under dark and AM 1.5 illumination.

Overall, the effects of silane passivation and c-TiO_2 layer on the cell efficiency (η) and the short-circuit current density (J_{sc}) were moderate under the simulated AM 1.5 solar spectrum. From the comparison of the fill factor (*FF*) between D1 and D2 (or between D3 and D4), the silane treatments did not affect the *FF*. However, there was a noticeable increase of the *FF* when the c-TiO_2 layer (in D3 or D4) was used. Another noticeable change is the open-circuit voltage (V_{oc}). The V_{oc} of D1 improved from 639 mV to 678 mV (D2) after silane treatment; it improved to 651 mV (D3) after employing a c-TiO_2 layer. The highest V_{oc} of 681 mV was achieved in D4 when both the silane treatment and the c-TiO_2 layer were used during the DSSCs fabrication. These results may imply that both the silane treatment and the c-TiO_2 layer could improve the V_{oc}, which is typically associated with reduced recombination.

For DSSCs based on organic dyes, the recombination reaction is a significant limiting factor to the DSSC performance. The goal of this paper is to understand the recombination in the DSSC based on organic sensitizer, which may help us for the future organic dye design. We focus our discussion on the effects of surface passivation on recombination reaction. The recombination in the DSSC has been investigated by the analysis of the dark current, the open-circuit voltage (V_{oc})−light intensity (Φ_0) dependence, and the transient photovoltage and photocurrent measurement.

Table 1. Solar Cell Parameters of DSSCs under AM 1.5 Illumination

no.	description	η (%)	J_{sc} (mA cm^{-2})	V_{oc} (mV)	FF (%)
D1	no c-TiO_2/ no silane	4.43 ± 0.17	10.3 ± 0.39	639 ± 2	67.1 ± 0.2
D2	no c-TiO_2/ silane	4.62 ± 0.12	10.2 ± 0.22	678 ± 3	66.8 ± 0.8
D3	c-TiO_2/no silane	4.72 ± 0.05	10.4 ± 0.12	651 ± 1	69.3 ± 0.1
D4	c-TiO_2/ silane	4.63 ± 0.13	9.62 ± 0.21	681 ± 4	70.2 ± 0.1

3.3. Dark Current Analysis. The J–V curves in the dark for the four devices are shown in Figure 2. (See the Supporting Information, Figure S4, for enlarged plot of the dark current). The dark current of DSSC is the measurement of the electrochemical overpotential of I_3^- reduction.[4,6] In the dark, the TiO_2 is generally insulating; the dark current is likely to take the path of the least overall resistance, which, in this case, is through the FTO surface to the electrolyte.[4] With no c-TiO_2 layer in D1 or D2, the onset of the dark current is rising at ~0.2 V; when the c-TiO_2 layer is introduced in D3 and D4, the onset potential for I_2 reduction shifts from ~0.2 V to ~0.4 V. The result indicates that the back electron transfer (recombination) from the FTO surface to the electrolyte is successfully blocked by the c-TiO_2 layer, which reduces the internal electron leakage from FTO to the electrolyte. Meanwhile, the c-TiO_2 layer also improves the shunt resistance, which explains the improved fill factor of D3 and D4 cells (Table 1).[24−26]

When the applied potential is over the flatband potential of the TiO_2, the TiO_2 film starts to become conductive. The high surface area of the TiO_2 film may boost the rapid I_3^- reduction (i.e., recombination) at the TiO_2 surface/electrolyte interface, which leads to rapid increase of the dark current. As shown in Figure 2, at high potential, the dark current of the photovoltaic cells after silane treatment (D2 and D4) is noticeably reduced compared with the samples without silane treatment, indicating that both silane and c-TiO_2 treatments are effective on suppressing recombination at TiO_2 and FTO in the devices.[27] To clarify the role of bare FTO electrode on the dark current, we have assembled a device without TiO_2 electrode, i.e. a device with the structure of FTO/electrolyte/Pt:FTO. In this case, the reduction of I_3^- species is purely at the FTO electrode surface. The dark IV of this device (see the Supporting Information, S4) is much smaller than those of DSSCs with TiO_2 electrodes, suggesting that the onset of the dark current is largely from the reduction of I_3^- species at TiO_2 photoanode.

3.4. Open-Circuit Voltage (V_{oc})–Light Intensity (Φ_0) Behavior. The relationship between V_{oc} and log(Φ_0) is plotted in Figure 3. On the basis of a model that considers several recombination mechanisms (including recombination involving electrons in both TiO_2 conduction band and trapping states), the slope of the linear fit of V_{oc}–log(Φ_0) is described using the following equation

$$\frac{dV_{oc}}{d\log \Phi_0} = \frac{2.3}{\beta}\frac{kT}{q}$$

where β is the ideality factor related to recombination involving the band gap surface states, Φ_0 is the light intensity, k is Boltzmann constant, q is elementary charge, and T is the absolute temperature.[28−30] In the ideal case (β = 1), only electrons in the conduction band of TiO_2 recombine with the I_3^- species, and the slope is 59 mV/decade; in a case where the electrons from the TiO_2 surface trapping states are involved in the recombination reaction, the slope is larger than the value of 59 mV/decade.

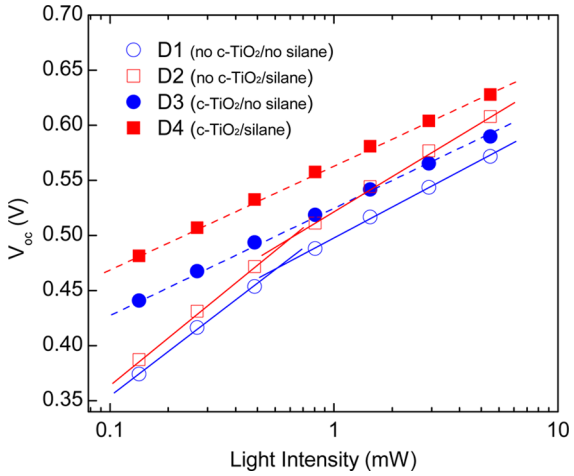

Figure 3. Open-circuit voltage (V_{oc}) of the DSSCs as a function of light intensity (Φ_0).

For D1 without silane and c-TiO_2 layer, two distinguished linear regions are observed in the V_{oc} v.s. log(Φ_0) plot. The linear fit of two regions gives slopes of 154 mV/decade (at low light intensity) and 106 mV/decade (at high light intensity). This result implies that there are two recombination pathways in the DSSC based on CDNA organic sensitizer without passivation of the TiO_2 and FTO surfaces. In D2, the TiO_2 surface is coated by a monolayer of alkyl chains, which reduces the contact between electrolyte and TiO_2 surface. Compared to D1, D2 shows similar V_{oc}–log(Φ_0) behavior. The V_{oc} vs. log(Φ_0) curve of this device is fitted with two linear regions, and the slopes of 164 mV/decade and 123 mV/decade at low and high light intensities are observed, respectively. However, the V_{oc} of D2 is higher than that of D1 at any given light intensity, particularly at the high light intensity. For D3 with only c-TiO_2 layer, the contacts between the FTO electrodes and the electrolyte are blocked. In the V_{oc}–log(Φ_0) curve of the device, the V_{oc} at the low intensity increases dramatically compared with those of D1 and D2 (i.e., cells without the c-TiO_2 layer). As a consequence, a linear relation between V_{oc} and log(Φ_0) is observed in the whole range of the light intensity measured. The linear fit of the curve gives slope of 94.7 mV/decade, smaller than those of D1 and D2. For D4 with silane treatment and c-TiO_2 layer, in which the contacts at both TiO_2/electrolyte and FTO/electrolyte interfaces are passivated, a large increase of V_{oc} is observed over the measurement light intensity range, and the linear fit of the V_{oc}–log(Φ_0) curve gives a slope of 93.5 mV/decade.

To summarize the observed V_{oc}–Φ_0 behavior of the four devices, the use of c-TiO_2 layer on FTO electrode leads to improved V_{oc}, and the improvement is more prominent at low light intensity; on the other hand, the silane passivation of TiO_2 photoanode also leads to improved V_{oc}, but the effect is more significant at high light intensity; collectively, use of both silane and c-TiO_2 in device fabrication yields the highest V_{oc} at the

measured light intensity range. These results can be rationalized by the following assumption. At the low light intensity, recombination between electrons in FTO electrode and I_3^- species in the electrolyte is more pronounced compared to that at the TiO_2/electrolyte interface, largely due to the small number of photoinjected electrons; on the contrary, the number of photoinjected electrons in TiO_2 film increases exponentially with the increase of light intensity, and the recombination at TiO_2/electrolyte interface becomes more important at high light intensity. Recombination at both TiO_2/electrolyte and FTO/electrolyte interfaces would affect the V_{oc} vs. Φ_0 behavior,[31,32] and the observed two linear regions in D1 and D2 can be attributed to the recombination reactions at both interfaces. Compared to D1, the silane passivation of TiO_2 in D2 blocks recombination at TiO_2 surface, which leads to the reduction of the overall recombination. Since the recombination at TiO_2/electrolyte is more significant at high light intensity, the reduction of the recombination is more pronounced at high light intensity after silane passivation of TiO_2. For D3 with only c-TiO_2 layer treatment, the recombination at TiO_2 occurs, while the recombination at FTO is blocked. As a consequence, the overall recombination is dominated by the recombination at the TiO_2/electrolyte interface. In this case, a single slope may be observed in the linear fit of the V_{oc}–log(Φ_0) over the measured range of light intensity, baed on a model considering the recombination at both the TiO_2 conduction band and the surfacing trapping states.[28] From the comparison with D1, the V_{oc} of D3 improved within the whole light intensity region, and larger improvement is observed at low light intensity, in consistence with blocking the major recombination event at FTO/electrolyte interface. For D4 with both silane treatment and c-TiO_2 layer, recombination at both FTO surface and TiO_2 surface are blocked, which leads to the highest V_{oc} at any given light intensity among all four samples. Further, the nearly identical slopes of D4 (93.5 mV/decade) and D3 (94.7 mV/decade) indicate that when recombination at FTO is blocked, the silane treatment on the TiO_2 film does not change the recombination mechanism, which is presumably through the surface trapping states in the TiO_2 film.

3.5. Transient Photovoltage and Photocurrent Measurement. The dark current characteristics and the V_{oc} - Φ_0 behavior provide valuable qualitative information on the electron recombination. To further quantitatively investigate the electron transport behavior in the DSSCs based on organic dyes, we have measured the transient photovoltage and photocurrent of the devices to evaluate the electron recombination lifetime (τ_e), the diffusion coefficient (D_{eff}), and the diffusion length (L).

The electron recombination depends on the incident light intensity, and more specifically, on the quasi-Fermi level within the TiO_2 band gap under illumination.[33] Because V_{oc} is determined by the difference between the quasi-Fermi level under illumination and the energy level of the redox couple,[34] the logarithm of τ_e as a function of V_{oc} is shown in Figure 4.

For each device with different surface passivation, the semilog τ_e–V_{oc} curve can be fitted with two linear regions. The slopes of the two linear regions are noticeably different for the samples without the c-TiO_2 layer (D1 and D2); on the other hand, the semilog τ_e–V_{oc} curves for the samples with the c-TiO_2 layer (D3 and D4) are nearly linear over the whole V_{oc} range, and only minor difference is observed in the slopes of the two linear regions. This can be ascribed to the similar

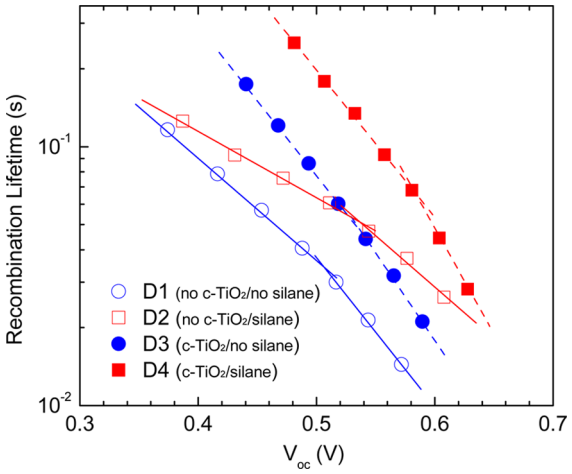

Figure 4. Electron recombination lifetime (τ_e) as a function of open-circuit voltage (V_{oc}).

explanation as the nonideal behavior of V_{oc}- Φ_0 behavior, i.e., the recombination is dominated by the FTO/electrolyte interface at low light intensity for the samples without the c-TiO_2 layer (D1 and D2). For understanding the effects of silane passivation of the TiO_2 surface, we first compare the recombination lifetime of D1 and D2 (i.e., devices without the c-TiO_2 layer) in Figure 4. At the high light intensity region (i.e., large V_{oc}), the silane treatment of the TiO_2 film substantially suppresses the recombination in the device; the electron recombination lifetime in D2 is several times longer than that in D1 at V_{oc} around 0.6 V. The suppression of recombination by silane treatment becomes less prominent at the low light intensity (i.e., small V_{oc}), and the semilog τ_e–V_{oc} curves of D1 and D2 start to merge together. This is a strong indication that the recombination is not only affected, but dominated by the FTO/electrolyte interface at low light intensity. For D3 and D4 with the c-TiO_2 layers, the recombination at the FTO/electrolyte interface is blocked; the back reactions at the TiO_2/electrolyte interface are the major contribution to the overall recombination of the devices in the whole light intensity region. In this case, silane treatment of the TiO_2 film is very effective on reducing recombination, since the τ_e of D4 is noticeably longer than that of D3. Moreover, the nearly identical slopes of the two curves in Figure 4 confirm that the mechanism and the order of the recombination reaction do not change after the silane treatment (i.e., the recombination is dominated by the TiO_2/electrolyte interface). These results indicate that both silane treatment and the c-TiO_2 layer can reduce the electron recombination in the DSSCs based on the organic sensitizer.

The surface properties of TiO_2 and FTO can affect not only the recombination rate but also the transport properties of electrons in DSSCs.[4] In Figure 5, we plot the diffusion coefficient (D_{eff}) derived from the photocurrent decay measurement at the short-circuit condition (see Experimental Section for details) as a function of V_{oc}. The devices without the silane treatment (D1 and D3) have similar values of D_{eff} over the measured V_{oc} range, whereas the D_{eff} of the devices with the silane treatment (D2 and D4) are also comparable. Overall, the silane treatment of the TiO_2 surface leads to lower D_{eff}, suggesting that the electron transport is hindered by the surface passivation of the TiO_2 film. This is likely due to the retarded regeneration of the photoexcited organic dye

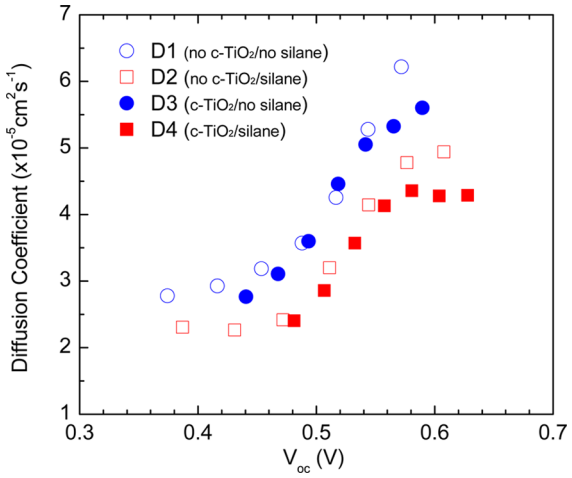

Figure 5. The electron diffusion coefficient (D_{eff}) as a function of open-circuit voltage (V_{oc}).

molecules by the silane coating.[5] Further, the data in Figure 5 indicates that the presence of the c-TiO_2 layer does not alter the overall electron transport of the DSSCs based on organic dyes in the measured range of V_{oc}.

Figure 6 shows the diffusion lengths (L) calculated from the τ_e and the D_{eff} data as a function of V_{oc}. In general, the diffusion

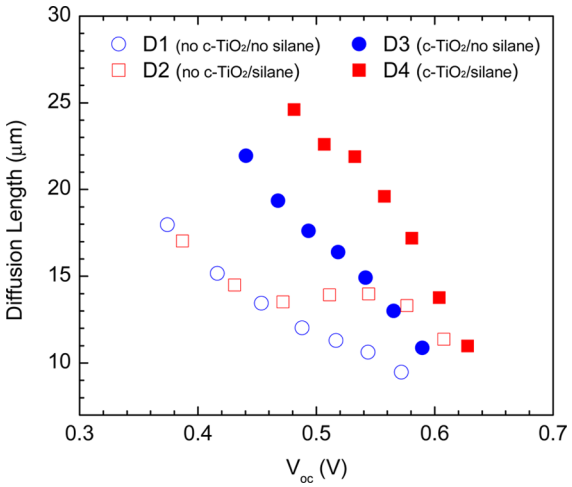

Figure 6. Electron diffusion length (L) as a function of open-circuit voltage (V_{oc}).

lengths of all four samples decrease with the increase of V_{oc} (i.e., the increase of the light intensity). For devices without the c-TiO_2 layers (D1 and D2), the recombination reactions occur at both the FTO/electrolyte and the TiO_2/electrolyte interfaces in D1, whereas the recombination reaction at the TiO_2/electrolyte interface is significantly reduced in D2. In the high V_{oc} region, the recombination at the FTO/electrolyte is relatively minor, and the silane passivation of TiO_2 in D2 leads to much longer diffusion length compare to that of D1 without the silane treatment; in the low V_{oc} region, the recombination at the FTO/electrolyte becomes dominant, and the diffusion lengths of D1 and D2 are comparable. For the samples with the c-TiO_2 layers, in which the recombination at the FTO/electrolyte interface is reduced substantially, the diffusion lengths are longer than that in the samples without the c-TiO_2 layer in the low V_{oc} region (i.e., low light intensity). At the high V_{oc}, the benefit of the c-TiO_2 layer starts to diminish for the devices with silane treatment (i.e., D2 and D4). In this situation, the silane treatment of the TiO_2 film has the significant advantage to block the primary recombination pathways (i.e., between the electrons in TiO_2 and I_3^- in electrolyte).

For DSSC based on the organic dye CDNA and the I^-/I_3^- redox couple, the suppression of recombination at the FTO surface is less significant at the high light intensity because the recombination is dominated by the TiO_2 surface. When the light intensity is low, the electron loss at the FTO surface becomes significant, and the addition of a c-TiO_2 layer can reduce the electron recombination significantly. The situation is quite different from the DSSC based on ruthenium dye N719, in which no such significant suppression of recombination by the c-TiO_2 layer is observed.[35] The difference may be ascribed to the chemical structures of N719 and CDNA. The N719 dye molecule (see the Supporting Information, Figure S5, for structure) has two carboxylate groups compared with only one carboxylate group in dye CDNA, which may suggest that there is stronger interaction between the FTO surface and dye N719.[24,36] Further, the large size of the ruthenium dye may physically separate the injected electrons in FTO and the I_3^- species in the electrolyte.[24] Consequently, the recombination at the FTO surface can be blocked by the ruthenium dye molecule. For future organic dye design, an organic dye with a bulky structure and possibly more anchoring groups will be beneficial on reducing the recombination loss at the FTO/electrolyte interface.

4. CONCLUSIONS

In conclusion, the recombination reactions at the FTO/electrolyte and the TiO_2/electrolyte interfaces are investigated using two surface passivation approaches of silane treatment and c-TiO_2 layer deposition in DSSCs based on a donor-π-acceptor dye and I^-/I_3^- redox couple. The dark current characteristics and the open-circuit voltage (V_{oc})-light intensity (Φ_0) behavior reveals that the recombination at the surface of TiO_2 is successfully suppressed by the silane treatment, and the recombination at the FTO surface can be reduced by the c-TiO_2 layer. The electron recombination lifetime (τ_e), the diffusion coefficient (D_{eff}), and the diffusion length (L) extracted from the transient photovoltage and photocurrent measurement indicate that under high photovoltage (i.e., high light intensity) the recombination is dominated by the TiO_2/electrolyte interface, and the passivation of the TiO_2 surface using silane treatment can suppress recombination significantly. On the other hand, incorporation the c-TiO_2 layer contribute little on reducing the total recombination at high light intensity, but can improve the fill factor through increasing the cell shunt resistance. Furthermore, the recombination at the FTO/electrolyte becomes significant at low light intensity, and this recombination can be effectively blocked by the c-TiO_2 layer. These results indicate that the passivation of the TiO_2 surfaces using silane treatment blocks the recombination substantially in the dye-sensitized solar cells based on organic dye CDNA. Our studies suggest that the method of silane passivation could be very useful for effectively blocking the recombination at the TiO_2/electrolyte interface in DSSCs based on organic sensitizers and/or fast redox couples (e.g., ferrocene/ferrocenium).

dx.doi.org/10.1021/am404984g | ACS Appl. Mater. Interfaces 2014, 6, 1926−1932

■ ASSOCIATED CONTENT

Supporting Information

Energetics of the dye, I^-/I_3^- redox, and TiO_2 photoanode, FTIR spectra of TiO_2 and TiO_2 passivated with silane, SEM image of the cross-section of photoanode, enlarged view of the dark current, chemical structure of N719. This material is available free of charge via the Internet at http://pubs.acs.org.

■ AUTHOR INFORMATION

Corresponding Authors

*E-mail: mswong@hkbu.edu.hk. Tel.: (852) 3411-7069. Fax: (852) 3411-7348.

*E-mail: Zhengtao.Zhu@sdsmt.edu. Tel.: (605) 394-2447. Fax: (605) 394-1232.

Author Contributions

The manuscript was written through contributions of all authors. All authors have given approval to the final version of the manuscript.

Notes

The authors declare no competing financial interest.

■ ACKNOWLEDGMENTS

This research was supported by the National Science Foundation (Grant Number: EPS-0903804), the National Aeronautics and Space Administration (Cooperative Agreement Number: NNX10AN34A), the Research Corporation Cottrell College Science Award (Award 10597), and the State of South Dakota. The work at Hong Kong Baptist University is supported by the Institute of Molecular Functional Materials, a grant from the University Grants Committee, Areas of Excellence Scheme (AoE/P-03/08), and a grant from the Research Grants Council (HKBU 203212).

■ REFERENCES

(1) O'Regan, B.; Grätzel, M. *Nature* **1991**, *353*, 737−740.

(2) Yella, A.; Lee, H.-W.; Tsao, H. N.; Yi, C.; Chandiran, A. K.; Nazeeruddin, M. K.; Diau, E. W.-G.; Yeh, C.-Y.; Zakeeruddin, S. M.; Grätzel, M. *Science* **2011**, *334*, 629−634.

(3) Hardin, B. E.; Snaith, H. J.; McGehee, M. D. *Nat. Photon.* **2012**, *6*, 162−169.

(4) Gregg, B. A.; Pichot, F.; Ferrere, S.; Fields, C. L. *J. Phys. Chem. B* **2001**, *105*, 1422−1429.

(5) Feldt, S. M.; Cappel, U. B.; Johansson, E. M. J.; Boschloo, G.; Hagfeldt, A. *J. Phys. Chem. C* **2010**, *114*, 10551−10558.

(6) Richards, C. E.; Anderson, A. Y.; Martiniani, S.; Law, C.; O'Regan, B. C. *J. Phys. Chem. Lett.* **2012**, *3*, 1980−1984.

(7) Li, T. C.; Góes, M. S.; Fabregat-Santiago, F.; Bisquert, J.; Bueno, P. R.; Prasittichai, C.; Hupp, J. T.; Marks, T. J. *J. Phys. Chem. C* **2009**, *113*, 18385−18390.

(8) Palomares, E.; Clifford, J. N.; Haque, S. A.; Lutz, T.; Durrant, J. R. *J. Am. Chem. Soc.* **2003**, *125*, 475−482.

(9) Jiang, D. l.; Hao, Y. Q.; Shen, R. J.; Ghazarian, S.; Ramos, A.; Zhou, F. M. *ACS Appl. Mater. Interfaces* **2013**, *5*, 11906−11912.

(10) Pothan, L. A.; George, J.; Thomas, S. *Compos. Interfaces* **2002**, *9*, 335−353.

(11) Spivack, J.; Siclovan, O.; Gasaway, S.; Williams, E.; Yakimov, A.; Gui, J. *Sol. Energy Mater. Sol. Cells* **2006**, *90*, 1296−1307.

(12) Cameron, P. J.; Peter, L. M. *J. Phys. Chem. B* **2003**, *107*, 14394−14400.

(13) Yamaguchi, T.; Tobe, N.; Matsumoto, D.; Arakawa, H. *Chem. Commun.* **2007**, 4767−4769.

(14) Bach, U. Solid-State Dye-Sensitized Mesoporous TiO_2 Solar Cells. *Ph.D. Thesis*, The Swiss Federal Institute of Technology, Lausanne, Switzerland, 2000.

(15) Wang, X. X.; He, G. F.; Fong, H.; Zhu, Z. T. *J. Phys. Chem. C* **2013**, *117*, 1641−1646.

(16) Wang, X. X.; Karanjit, S.; Zhang, L. F.; Fong, H.; Qiao, Q. Q.; Zhu, Z. T. *Appl. Phys. Lett.* **2011**, *98*, 082114.

(17) Barnes, P. R. F.; Miettunen, K.; Li, X.; Anderson, A. Y.; Bessho, T.; Gratzel, M.; O'Regan, B. C. *Adv. Mater.* **2013**, *25*, 1881−1922.

(18) Enache-Pommer, E.; Boercker, J. E.; Aydil, E. S. *Appl. Phys. Lett.* **2007**, *91*, 123116.

(19) Schlichthorl, G.; Park, N. G.; Frank, A. J. *J. Phys. Chem. B* **1999**, *103*, 782−791.

(20) Mukherjee, K.; Teng, T.-H.; Jose, R.; Ramakrishna, S. *Appl. Phys. Lett.* **2009**, *95*, 012101.

(21) Wang, X. X.; Guo, L.; Xia, P. F.; Wong, M. S.; Zhu, Z. T. *J. Mater. Chem. A* **2013**, *1*, 13328−13336.

(22) Morris, A. J.; Meyer, G. J. *J. Phys. Chem. C* **2008**, *112*, 18224−18231.

(23) McCarthy, S. A.; Davies, G.-L.; Gun'ko, Y. K. *Nat. Protoc.* **2012**, *7*, 1677−1693.

(24) Burke, A.; Ito, S.; Snaith, H.; Bach, U.; Kwiatkowski, J.; Gratzel, M. *Nano Lett.* **2008**, *8*, 977−981.

(25) Nelson, J. *The Physics of Solar Cells*; Imperial College Press: London, 2003.

(26) Hore, S.; Kern, R. *Appl. Phys. Lett.* **2005**, *87*, 263504.

(27) Zhang, Z.; Zakeeruddin, S. M.; O'Regan, B. C.; Humphry-Baker, R.; Grätzel, M. *J. Phys. Chem. B* **2005**, *109*, 21818−21824.

(28) Salvador, P.; Hidalgo, M. G.; Zaban, A.; Bisquert, J. *J. Phys. Chem. B* **2005**, *109*, 15915−15926.

(29) Zhang, C.; Chen, S.; Tian, H.; Huang, Y.; Huo, Z.; Dai, S.; Kong, F.; Sui, Y. *J. Phys. Chem. C* **2011**, *115*, 8653−8657.

(30) Jennings, J. R.; Wang, Q. *J. Phys. Chem. C* **2010**, *114*, 1715−1724.

(31) Cameron, P. J.; Peter, L. M. *J. Phys. Chem. B* **2005**, *109*, 7392−7398.

(32) Cameron, P. J.; Peter, L. M.; Hore, S. *J. Phys. Chem. B* **2005**, *109*, 930−936.

(33) Mohammadpour, R.; Iraji zad, A.; Hagfeldt, A.; Boschloo, G. *Phys. Chem. Chem. Phys.* **2011**, *13*, 21487−21491.

(34) Frank, A. J.; Kopidakis, N.; van de Lagemaat, J. *Coord. Chem. Rev.* **2004**, *248*, 1165−1179.

(35) Ito, S.; Liska, P.; Comte, P.; Charvet, R.; Pecchy, P.; Bach, U.; Schmidt-Mende, L.; Zakeeruddin, S.; Kay, A.; Nazeeruddin, M.; Grätzel, M. *Chem. Commun.* **2005**, *34*, 4351.

(36) Zhu, R.; Jiang, C.-Y.; Liu, B.; Ramakrishna, S. *Adv. Mater.* **2009**, *21*, 994−1000.